ZERO-IG: Zero-Shot Illumination-Guided Joint Denoising and Adaptive Enhancement for Low-Light Images – Supplemental Materials –

Yiqi Shi [1*], Duo Liu [1*], Liguo Zhang [1†], Ye Tian [2], Xuezhi Xia [1,3], Xiaojing Fu [1]
[1] School of Computer Science and Technology, Harbin Engineering University
[2] Hangzhou Institute of Technology, Xidian University
[3] Wuhan Digital Engineering Research Institute
{shiyiqi, liu_duo, zhangliguo, fuxiaojing }@hrbeu.edu.cn,
tianye@xidian.edu.cn, xiaxuezhi709@gmail.com

Abstract

This is the Supplemental Materials for the paper: "ZERO-IG: Zero-Shot Illumination-Guided Joint Denoising and Adaptive Enhancement for Low-Light Images". Initially, our VILNC dataset is introduced in Section 1. Besides, Section 2 offers computational efficiency and more visual comparisons, featuring low-light images with real noise, varying brightness levels from the VILNC dataset, and low-light images with synthetic noise. It is obvious that the proposed ZERO-IG achieves the best performance, further verifying our superiority. Finally, additional ablation experiments are detailed in Section 3.

1. VILNC Dataset

(a) Indoor Dark I (b) Indoor Dark II (c) Indoor Dark III (d) Indoor Light (e) Outdoor Dark (f) Outdoor Light

Figure 1. Sample images in our VILNC dataset. Each row in the first three columns contains low-light images at three different brightness levels from the same indoor scene. The fourth column has the corresponding indoor normal-light reference images. The last two columns feature low-light images and their corresponding normal-light reference images from outdoor scenes.

Creating datasets for Low-Light Image Enhancement (LLIE) training and evaluation poses significant challenges. Most existing datasets are derived by synthesizing images or altering camera settings. Frequently, their capacity to accurately

---

*Equal Contribution.
†Corresponding Author.

represent real-world conditions is limited. Methods trained on synthetic images may introduce artifacts and color bias when processing real-world images. Furthermore, images captured by adjusting exposure time and ISO settings often lack the complete details and especially noise present in genuine low-light scenes.

Our new Varied Indoor Luminance & Nightscapes Collection (VILNC) dataset comprises 500 real-world low-light images captured using a Canon EOS 550D, including 460 indoor and 40 outdoor scenes. Figure 1 displays a selection of images from this dataset. Specifically, the indoor segment features low-light images at three distinct brightness levels. We adjusted the Mijia Desk Lamp 1S to a color temperature of 6496, and brightness levels of 10, 30, and 50, to simulate varying degrees of low-light. Images captured in full-light conditions serve as normal-light reference images. The ISO value was set to 400 and the exposure time to 1. In the outdoor portion, night-time images are classified as low-light. The ISO for these images is set to 1600 with an exposure time of 1. Daytime images, used as normal-light references, have an ISO of 100 and an exposure time of 1/80. To prevent movement and ensure consistent framing, a tripod was used to stabilize the camera. Our VILNC dataset is available at `https://github.com/Doyle59217/ZeroIG`.

2. More Experimental Results

2.1. Computational Efficiency

Table 1 shows the comparisons of running time and model size across methods, averaged over 300 random images with a size of $600 \times 400 \times 3$ from the LOL-v2 [12] dataset.

Table 1. Comparisons of running time (RT) and model size (SIZE) on LOL-v2 [12] dataset.

Metrics	*Supervised Learning Methods*				*Unsupervised Learning Methods*			
	URtinex-Net	**LLFlow**	**SNR-aware**	**KinD++**	**SCI**	**PairLIE**	**RUAS**	**ZERO-IG**
RT(s)↓	0.2853	0.2231	0.1927	0.1725	**0.0005**	0.0065	0.0121	**0.0035**
SIZE(K)↓	340.11	4970.3	39135	9632.1	**0.2580**	341.72	**3.438**	86.572

2.2. Visual Comparison on Low-light Images with Real Noise

Figure 2 shows visual comparisons on our VILNC dataset. Compared to other methods, ZERO-IG consistently achieves stable enhancement results for real low-light images across various brightness levels. Figures 3, 4 and 5 additionally provide

(a) Input (b) LLFlow [9] (c) PairLIE [4] (d) RUAS [7] (e) SNR-aware [11] (f) SCI [8] (g) ZERO-IG

Figure 2. Visual comparisons on our VILNC dataset. The first three rows show the enhancement effects of indoor low-light scenes across various brightness levels. The last row shows the enhancement effect of an outdoor low-light scene.

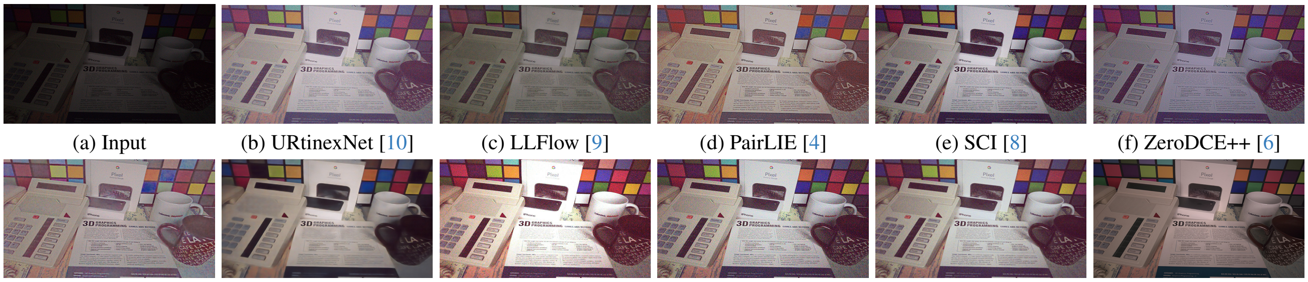

(a) Input (b) URtinexNet [10] (c) LLFlow [9] (d) PairLIE [4] (e) SCI [8] (f) ZeroDCE++ [6]
(g) KinD++ [13] (h) SNR-aware [11] (i) RUAS [7] (j) ZERO-IG-IE-Net (k) ZERO-IG (l) Ref

Figure 3. Visual comparison on a real noisy low-light image from the SIDD [1] dataset.

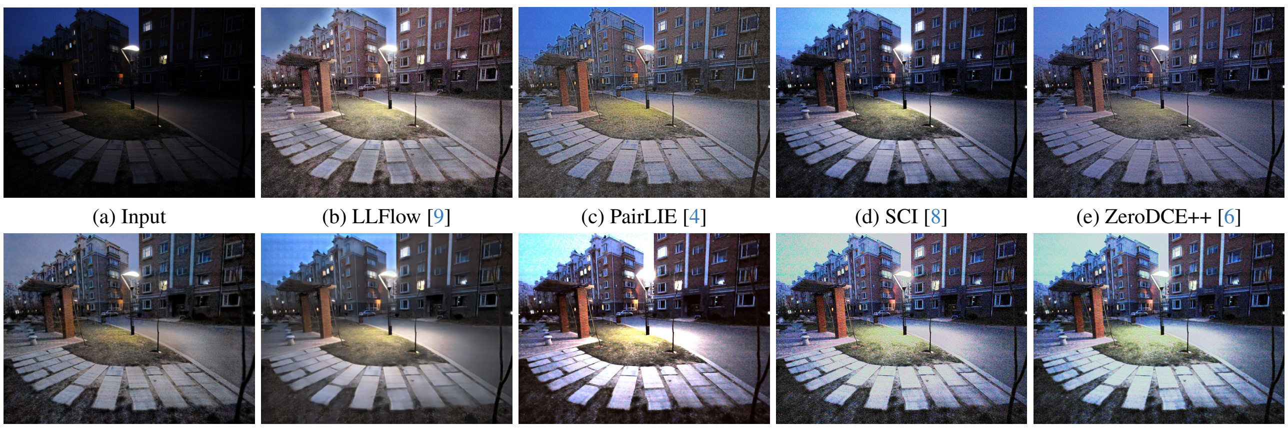

(a) Input (b) LLFlow [9] (c) PairLIE [4] (d) SCI [8] (e) ZeroDCE++ [6]
(f) KinD++ [13] (g) SNR-aware [11] (h) RUAS [7] (i) ZERO-IG-IE-Net (j) ZERO-IG

Figure 4. Visual comparison on a real noisy low-light image from the LIME [5] dataset.

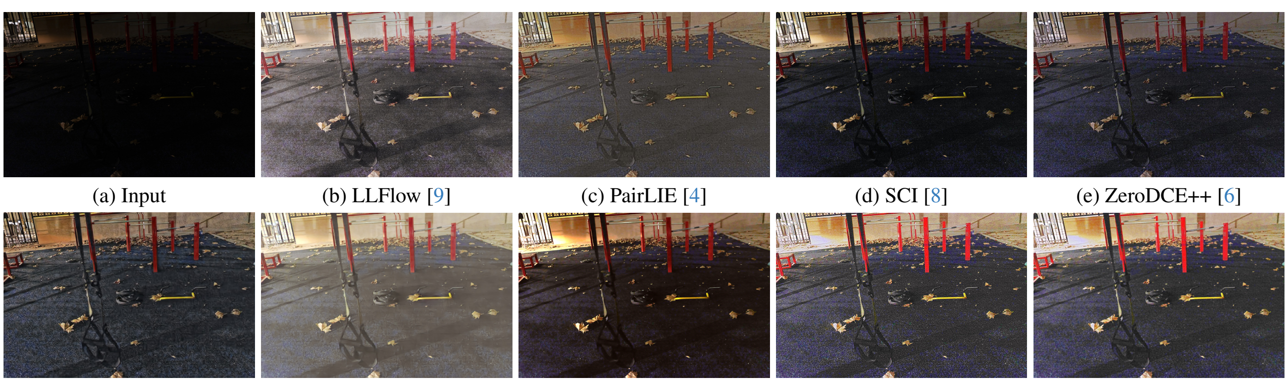

(a) Input (b) LLFlow [9] (c) PairLIE [4] (d) SCI [8] (e) ZeroDCE++ [6]
(f) KinD++ [13] (g) SNR-aware [11] (h) RUAS [7] (i) ZERO-IG-IE-Net (j) ZERO-IG

Figure 5. Visual comparison on a real noisy low-light image from the SID [3] dataset.

visual comparisons of real-world low-light images from the SIDD [1], LIME [5] and SID [3] datasets. It can be seen that our method outperforms others in terms of image brightness, contrast, color fidelity, and noise reduction.

2.3. Visual Comparison on Low-light Images with Synthetic Noise

To further demonstrate ZERO-IG's effectiveness, we introduced Gaussian, Salt-and-Pepper, Uniform, and Poisson noise types into the MIT-Adobe FiveK [2] dataset, respectively. Gaussian noise simulates random deviations in pixel values caused by factors such as thermal noise from electronic devices. We used a fixed Gaussian noise level σ of 10, indicating the standard deviation in the pixel value range [0, 255]. Salt-and-Pepper noise simulates data loss or signal interference in digital image

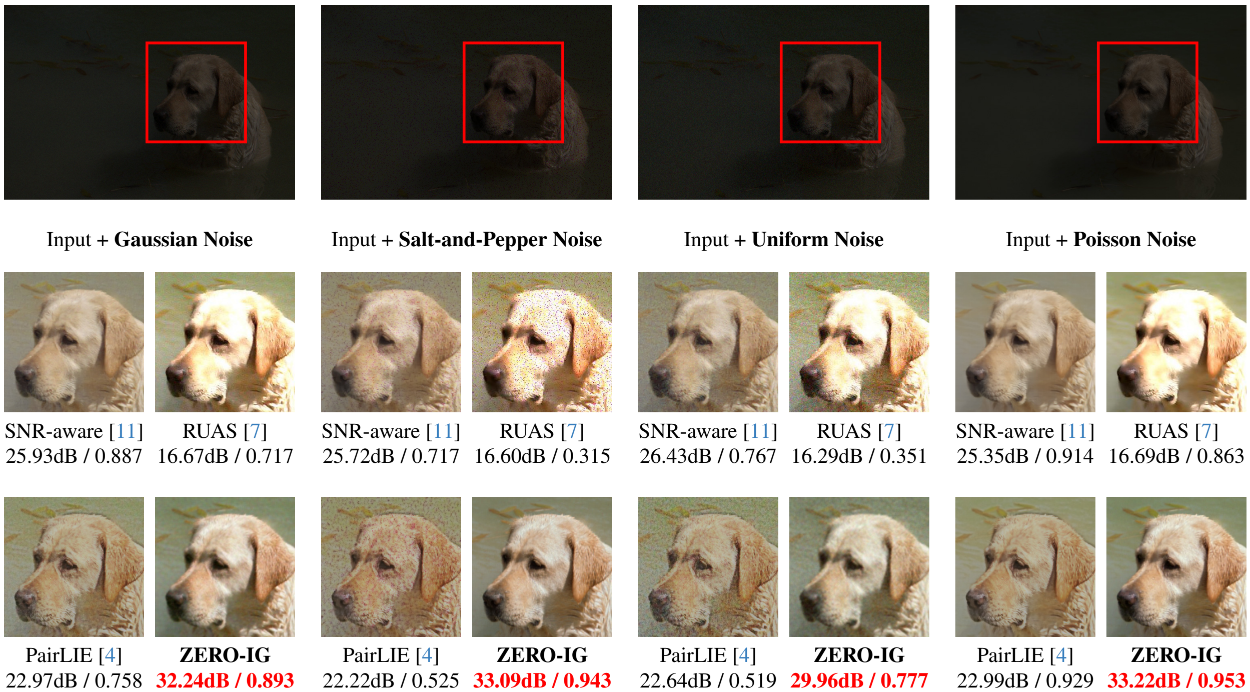

Figure 6. Visual comparisons on low-light images with synthetic noise. We provide **PSNR/SSIM** of each method w.r.t. clean ground-truth image. The best results are highlighted in **red**.

transmission. The value of some pixels in the low-light image were randomly set to be the highest (represented by white, i.e. ”salt”) or the lowest (represented by black, i.e. ”pepper”).

Uniform noise models the uniformly distributed random errors from sensor or environmental interference during image acquisition. We added uniformly distributed random noise, with an intensity range of -10 to 10, to all pixels of the low-light image. Poisson noise, often linked to image brightness, simulates random fluctuations in photon counts. A Poisson distributed noise matrix was generated based on the count of unique pixel values, and then added to the original image. As shown in Figure 6, our method effectively enhances low-light images affected by four types of synthetic noise, excelling in both visual and metric assessments.

3. Additional ablation experiments

Figure 7(a) illustrates the overall adjustment loss, showing the impact of various brightness coefficients α in IE-Net. Enlarging all pixels equally improves low-light image brightness but may lead to under-enhancement or over-exposure. Figure 7(b) displays the pixel-by-pixel adjustment loss, highlighting varying enhancement amplitudes for each pixel at different well-exposedness levels E in IE-Net. Figure 7(c) illustrates the principle behind the color loss in RD-Net. The color loss evaluates dominant color differences between images by eliminating texture and content comparisons. It ensures the denoised image retains the same color distribution as the noisy image, tolerating minor mismatches. Figure 7(d) presents our method's intermediate results, including the approximately equal to the noise-unaffected illumination $\tilde{S}$, noise-contaminated reflection R, binary denoising indicator D, noise n, and the final enhanced image $\hat{R}$.

We study the effect of the average brightness Y_H of the normal-light image in the overall adjustment loss and the well-exposedness level E in the pixel-by-pixel adjustment loss on the enhancement performance of our method. Five Y_H values (i.e., 0.3, 0.4, 0.5, 0.6, 0.7) were used to train our network, resulting in the models ZERO-IG$_{Y_H 0.3}$ to ZERO-IG$_{Y_H 0.7}$. Similarly, five E values (i.e., 0.5, 0.6, 0.7, 0.8, 0.9) led to models ZERO-IG$_{E0.5}$ to ZERO-IG$_{E0.9}$. Observations from Figure 8 and 9 show that ZERO-IG$_{Y_H 0.5}$ and ZERO-IG$_{E0.7}$ achieve pleasing brightness. Consequently, ZERO-IG$_{Y_H 0.5}$ and ZERO-IG$_{E0.7}$ were chosen as the final ZERO-IG model due to their better visual results.

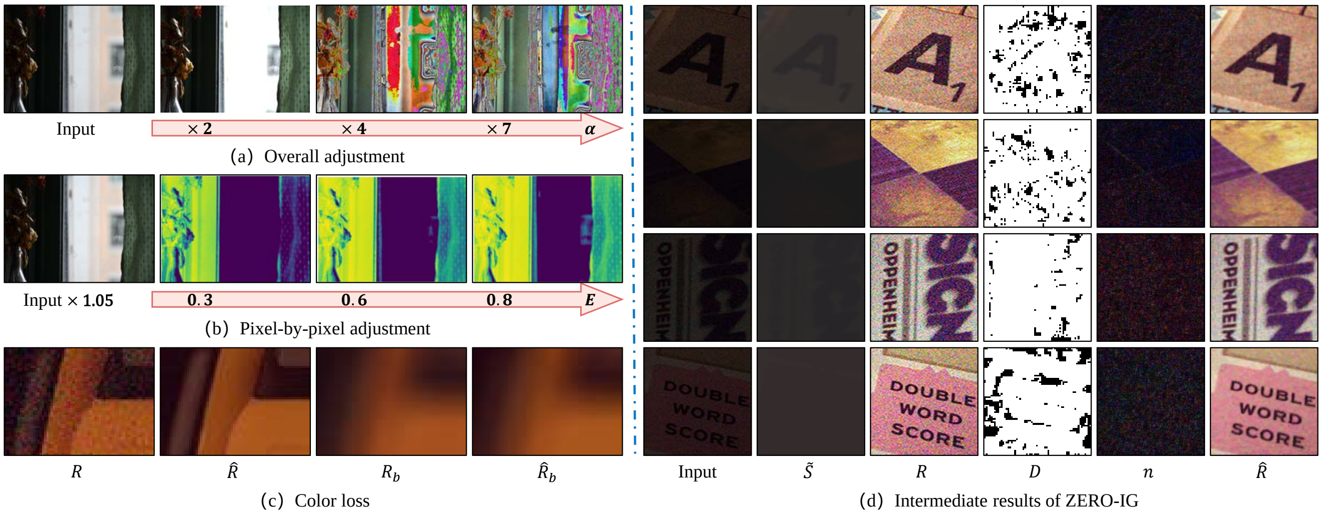

Figure 7. (a) Different brightness coefficients α in the overall adjustment loss. (b) Different well-exposedness levels E in the pixel-by-pixel adjustment loss. (c) Principle of the color loss. R_b and $\hat{R}_b$ represent the blurred versions of R and $\hat{R}$. (d) Intermediate results of ZERO-IG.

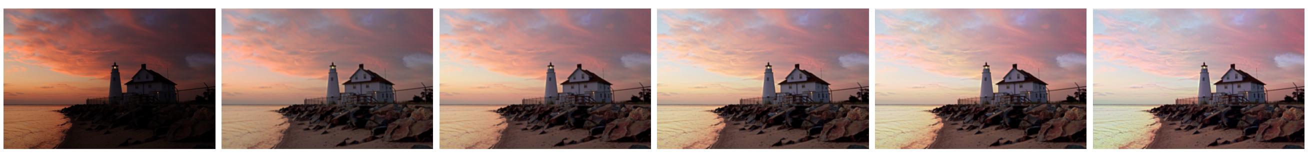

(a) Input | (b) ZERO-IG$_{Y_H 0.3}$ | (c) ZERO-IG$_{Y_H 0.4}$ | (d) ZERO-IG$_{Y_H 0.5}$ | (e) ZERO-IG$_{Y_H 0.6}$ | (f) ZERO-IG$_{Y_H 0.7}$

Figure 8. Visual comparison among the results generated by the ZERO-IG trained using different brightness of the normal-light image, Y_H, in the overall adjustment loss.

(a) Input | (b) ZERO-IG$_{E0.5}$ | (c) ZERO-IG$_{E0.6}$ | (d) ZERO-IG$_{E0.7}$ | (e) ZERO-IG$_{E0.8}$ | (f) ZERO-IG$_{E0.9}$

Figure 9. Visual comparison among the results generated by the ZERO-IG trained using different well-exposedness level, E, in the pixel-by-pixel adjustment loss.

References

[1] Abdelrahman Abdelhamed, Stephen Lin, and Michael S Brown. A high-quality denoising dataset for smartphone cameras. In *Proceedings of the IEEE/CVF Conference on Computer Vision and Pattern Recognition*, pages 1692–1700, 2018. 3

[2] Vladimir Bychkovsky, Sylvain Paris, Eric Chan, and Frédo Durand. Learning photographic global tonal adjustment with a database of input/output image pairs. In *Proceedings of the IEEE/CVF Conference on Computer Vision and Pattern Recognition*, pages 97–104, 2011. 3

[3] Chen Chen, Qifeng Chen, Jia Xu, and Vladlen Koltun. Learning to see in the dark. In *Proceedings of the IEEE/CVF Conference on Computer Vision and Pattern Recognition*, pages 3291–3300, 2018. 3

[4] Zhenqi Fu, Yan Yang, Xiaotong Tu, Yue Huang, Xinghao Ding, and Kai-Kuang Ma. Learning a simple low-light image enhancer from paired low-light instances. In *Proceedings of the IEEE/CVF Conference on Computer Vision and Pattern Recognition*, pages 22252–22261, 2023. 2, 3, 4

[5] Xiaojie Guo, Yu Li, and Haibin Ling. Lime: Low-light image enhancement via illumination map estimation. *IEEE Transactions on Image Processing*, 26(2):982–993, 2016. 3

[6] Chongyi Li, Chunle Guo, and Chen Change Loy. Learning to enhance low-light image via zero-reference deep curve estimation. *IEEE Transactions on Pattern Analysis and Machine Intelligence*, 44(8):4225–4238, 2021. 3

[7] Risheng Liu, Long Ma, Jiaao Zhang, Xin Fan, and Zhongxuan Luo. Retinex-inspired unrolling with cooperative prior architecture

search for low-light image enhancement. In *Proceedings of the IEEE/CVF Conference on Computer Vision and Pattern Recognition*, pages 10561–10570, 2021. 2, 3, 4

[8] Long Ma, Tengyu Ma, Risheng Liu, Xin Fan, and Zhongxuan Luo. Toward fast, flexible, and robust low-light image enhancement. In *Proceedings of the IEEE/CVF Conference on Computer Vision and Pattern Recognition*, pages 5637–5646, 2022. 2, 3

[9] Yufei Wang, Renjie Wan, Wenhan Yang, Haoliang Li, Lap-Pui Chau, and Alex Kot. Low-light image enhancement with normalizing flow. In *Proceedings of the AAAI Conference on Artificial Intelligence*, pages 2604–2612, 2022. 2, 3

[10] Wenhui Wu, Jian Weng, Pingping Zhang, Xu Wang, Wenhan Yang, and Jianmin Jiang. Uretinex-net: Retinex-based deep unfolding network for low-light image enhancement. In *Proceedings of the IEEE/CVF Conference on Computer Vision and Pattern Recognition*, pages 5901–5910, 2022. 3

[11] Xiaogang Xu, Ruixing Wang, Chi-Wing Fu, and Jiaya Jia. Snr-aware low-light image enhancement. In *Proceedings of the IEEE/CVF Conference on Computer Vision and Pattern Recognition*, pages 17714–17724, 2022. 2, 3, 4

[12] Wenhan Yang, Shiqi Wang, Yuming Fang, Yue Wang, and Jiaying Liu. From fidelity to perceptual quality: A semi-supervised approach for low-light image enhancement. In *Proceedings of the IEEE/CVF Conference on Computer Vision and Pattern Recognition*, pages 3063–3072, 2020. 2

[13] Yonghua Zhang, Xiaojie Guo, Jiayi Ma, Wei Liu, and Jiawan Zhang. Beyond brightening low-light images. *International Journal of Computer Vision*, 129:1013–1037, 2021. 3